http://dx.doi.org/10.5012/bkcs.2012.33.7.2168

# Relations between Resonance Structures in Photoionization Spectra in Three-Channel-Systems Studied by Multichannel Quantum Defect Theory

**Chun-Woo Lee**

*Department of Chemistry, Ajou University, Suwon 443-749, Korea. E-mail: clee@ajou.ac.kr*
*Received March 2, 2012, Accepted March 26, 2012*

Relations between fitted parameters for photoionization spectra both below and above the thresholds in the systems involving 3 channels are obtained using phase-shifted version of the multichannel quantum-defect theory. Analytical continuation of the photoionization cross sections in the form of $\langle\sigma_{\text{below}}\rangle_{\nu_{\text{below}}} = \sigma_{\text{above}}$ is examined using several representations.

**Key Words :** Phase-shifted MQDT, Threshold phenomena, Resonance structures, Interlopers

## Introduction

Threshold phenomena have drawn enormous attention,[1-3] since the energy dependence of the cross section near the threshold was first studied by Wigner.[4] Wigner demonstrated that energy dependence in the neighborhood of the threshold remains the same, apart from a constant, regardless of the specifics of reaction or reaction products as long as the long-range interaction of the product particles is the same. Because of such a generality, threshold phenomena have been of interest in many areas of physics and chemistry.[1,2,5-7] Since slow-moving near-threshold particles spend a long-time under the influence of any long-range potentials as they are departing, it is those potentials rather than any shorter-range ones that govern the threshold behaviors.

Wigner obtained the threshold laws for the attractive and repulsive Coulomb potentials and no long-range interaction. In the case of no long-range interaction, cross sections were determined only by the lowest angular momentum quantum number allowed as $\sigma \propto E^{(2l+1)/2}$ and were beautifully demonstrated in the photo-detachment spectra of anions.[8] For the attractive Coulomb potential, the cross section remains finite at the thresholds for all angular momentum quantum numbers as routinely observed in photoionization spectra of neutral species.[9-11] The effects of long-range potentials other than Coulomb and centrifugal ones, like a polarization potential $r^{-3}$ and $r^{-4}$ on the threshold laws are so diverse and have a number of interesting aspects to be summarized in a few sentences. For further details and additional topics such as *N*-body threshold laws, please refer to Refs. [1,11,12].

Threshold behaviors are also intensely studied in the multichannel quantum defect theory (MQDT) in order to treat the photo-absorption and photoionization spectra on an equal footing.[10,11] Such studies were mostly concentrated on the analytical continuity of base functions across the thresholds. The fact that the photoionization cross sections below the threshold averaged over resonances are equal to those of the total photoionization spectra just above the threshold, was repeatedly derived in the past[10,13] in the context of photoionization for the simple one-open-one-closed channel system except for the Dubau and Seaton's derivation given in Ref. [14], in which the authors suggested that general treatment can be given using the contracted matrix method. This kind of analytical continuation of the cross section below the threshold averaged over resonances to the one above the threshold is known as the Gailitis theorem.[15] Although studied extensively, there remain several interesting aspects in the analytical continuation across the threshold.

For the concreteness, let us restrict the system to the photoionization of the system involving 3 non-degenerate channels with the thresholds energies $I_i$ satisfying $I_1 < I_2 < I_3$. Let us call the corresponding thresholds the first, second and third thresholds, respectively. Let us also use the terms, limit interval 1, 2, 3, and 4 as shown in Figure 1. Limit interval 1 belongs to the photo-absorption regime. In limit interval 2, if the effect of an interloper dominates the spectra, the formalism developed by Connerade,[16] Cooke and Cromer[17] and Ueda[18] may be used to analyze the spectra. In limit interval 3, Beutler-Fano formula is usually used to fit the observed spectra. Table 1 shows resonance-resolved cross-section formulas and quantum-defect theory (QDT) parameters used to fit experimental data in all the limit intervals. Detailed description will be given in the following sections.

In limit interval 3, the system involves one closed and 2

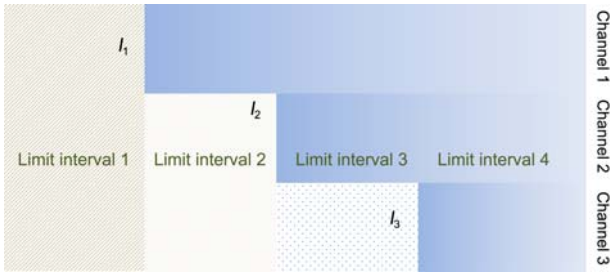


**Figure 1.** The three-channel-system with ionization energies ordered as $I_1 < I_2 < I_3$. Ranges of energy divided by $I_i$ are termed as limit intervals.

**Table 1.** Resonance-resolved cross-section formulas, QDT parameters used to fit experimental data and analytical continuation in 4 limit intervals

| | Limit interval 1 | Limit interval 2 | Limit interval 3 | Limit interval 4 |
|---|---|---|---|---|
| Photoionization cross section | $\sigma_{\mathrm{I}}$ | $\sigma_{\mathrm{II}}$ | $\sigma_{\mathrm{III}}$ | $\sigma_{\mathrm{IV}}$ |
| Resonance-Structure resolved formula | Discrete spectrum | $\sigma_0\frac{(\varepsilon_3+q_3)^2}{\varepsilon_3^2+1}\frac{(\varepsilon_{2\mathrm{eff}}+q_{2\mathrm{eff}})^2}{\varepsilon_{2\mathrm{eff}}^2+1}$ | $\sigma_{\mathrm{r1}}\frac{(\tilde{\varepsilon}_{\mathrm{r}}+\tilde{q}_{\mathrm{r}})^2}{\tilde{\varepsilon}_{\mathrm{r}}^2+1}+\sigma_{\mathrm{r2}}$ | No resonance $D(1+K^2)^{-1}D^{\mathrm{T}}$ |
| QDT parameters | $\begin{pmatrix} K'_{11} & K'_{12} & K'_{13} \\ K'_{12} & K'_{22} & K'_{23} \\ K'_{13} & K'_{23} & K'_{33} \end{pmatrix}$ | $\begin{pmatrix} 0 & K_{12} & K_{13} \\ K_{12} & 0 & K_{23} \\ K_{13} & K_{23} & 0 \end{pmatrix}$ | $\begin{pmatrix} 0 & 0 & \xi_{\mathrm{r}} \\ 0 & 0 & 0 \\ \xi_{\mathrm{r}} & 0 & 0 \end{pmatrix}$ | $\xi_{\mathrm{r}}$ |
| | $D'_1, D'_2, D'_3$ | $\mu_1(=0), \mu_2, \mu_3$ | $\mu^{\mathcal{E}}=\mu_3$ | $D_{\mathrm{r1}}, D_{\mathrm{r2}}, D_{\mathrm{r3}}$ |
| | $I_1, I_2, I_3$ | $D_1, D_2, D_3$ | $D_{\mathrm{r1}}, D_{\mathrm{r2}}, D_{\mathrm{r3}}$ | $I_1, I_2, I_3$ |
| | | $I_1, I_2, I_3$ | $I_3$ | |
| Analytical continuation | | $\langle\sigma_{\mathrm{I}}\rangle_{\nu_1}=\sigma_{\mathrm{II}}$ | $\langle\sigma_{\mathrm{II}}\rangle_{\nu_2}=\sigma_{\mathrm{III}}$ | $\langle\sigma_{\mathrm{III}}\rangle_{\nu_3}=\sigma_{\mathrm{IV}}$ |

open channels. The presence of more than one open channel leads to changes in the resonance frame from that of the limit interval 2. This specific problem was extensively studied in Ref. [19] (hereafter referred as LK) mostly using the incoming wave channel basis functions. For the total cross sections, the use of incoming waves is inconvenient because of the presence of complex numbers. Most of the formulas in LK were thus re-derived in terms of standing-wave channel basis functions. Because of the change in the resonance eigenframes for limit intervals 2 and 3, caution is needed in relating QDT parameters obtained from experimental data in fitting in different limit intervals. To obtain the relations between resonance structures in photoionization spectra in three-channel-systems is one of the main subjects of the present study. The relation between the spectral shapes of the autoionizing Rydberg series 3 below and above the second ionization limit, in particular, motivated this study. Channel 3 usually acts as an interloper to the auto-ionizing Rydberg series 2 in the second limit since, the line widths of interloper series 3 are much broader than those of the perturbed series 2 because of the normal decrease in the spectral width of Rydberg series as $n^{-3}$. Interloper series thus auto-ionizes much faster than the perturbed series and is thus hardly affected by series 2. Because of this, Rydberg series 3 is well defined in limit interval 2 and may be expected to be continued without much of a change to the same series in limit interval 3. On the other hand, previous study makes it clear that the line profile parameter is not an intrinsic property of the series, but is determined by the resonance structure of the system.[20,21] Since resonance structures or eigenframes are different both below and above threshold 2, it is expected that the line profile parameter also undergoes a change both below and above the second threshold. The relation between the line profile parameters of series 3 below and above the threshold of perturbed series is therefore worth pursuing. Since this problem turns out to be in close relation to the analytical continuation of the cross section, the research carried out on that subject will be presented. With respect to the present research work, Dubau and Seaton's contracted matrix method was useful and will be presented finally.

**Cross section Formula for the Perturbed Autoionizing Series by an Interloper.** If only one open channel is involved in the ionizing process by photon, the photoionization cross section can be described in terms of the transition dipole moment matrix **D** by a single term, $K|\mathbf{D}|^2(\equiv K|(\Psi|T|i)|^2)$ where, $T$ denotes the transition dipole operator; $|i)$ is the initial state wavefunction; $\Psi$ is the photoionizing state, the constant $K$ is given by $(4\pi^2\alpha\omega/3)$ with the fine-structure constant $\alpha$ and the photon energy $\hbar\omega$. Since, multichannel quantum defect theory (MQDT) is known to be the most powerful method for obtaining $\Psi$, let us briefly describe the MQDT description of $\Psi$.

If many channels are involved in the autoionization, the photo-ionizing wavefunction $\Psi$ can be expanded in terms of the standing-wave channel basis functions $\Psi_i$ as

$$\Psi=\Psi_1\cos\delta+\sum_{i\in Q}\Psi_i Z_i\cos\pi(\nu_i+\mu_i) \tag{1}$$

where, index 1 denotes the open channel and $Q$ denotes the set of closed channels; $Z_i$ are the expansion coefficients; $\cos\delta$ and $\cos\pi(\nu_i+\mu_i)$ are needed to make $\Psi$ energy normalized and will be defined below. For the range of ionization coordinate $R$ larger than some value $R_0$, channels are decoupled and the motion along $R$ in each decoupled channel is governed by the second-order differential equations whose solutions are given by the linear combinations of the regular and irregular base pair, say $f_j(R)$ and $g_j(R)$ for the $j$-th channel belonging to the threshold of ionization energy $I_j$. Channel basis functions $\Psi_i$ at energy $E$ can thus be written as;

$$\Psi_i=\sum_{j=1}^{3}\Phi_j(\omega)[f_j(R)\delta_{ji}-g_j(R)K_{ji}]\,,\quad (R>R_0), \tag{2}$$

where, $\Phi_j(\omega)$ are the wavefunctions composed of the ion core and the angular and spin part of the outer electron in the $j$-th channel and the coefficients $K_{ji}$ are called reactance matrix and describe the extent of the coupling from other

channels.

The expansion coefficients in (1) can be obtained from the boundary condition that $\Psi$ remains finite at $R \to \infty$ :[11]

$$\cos\pi(\nu_j+\mu_j)Z_j = -[(\tan\pi(\nu_j+\mu_j)+K^{cc})^{-1}K^{co}]_j \cos\delta, \quad (3)$$

where, $\nu_j$ is the effective quantum number defined by $E = I_j$ – Ryd/ $\nu_j^2$ ; $\cos\delta$ is related to the physical reactance matrix defined by $\mathbf{K} = K^{oo} - K^{oc}(\tan\beta + K^{cc})^{-1}K^{co}$ as $(1+\mathbf{K}^2)^{-1/2}$ for the one open-channel system. In the phase-shifted MQDT, the phases of $f_j$ and $g_j$ are shifted by $\pi\mu_j$ as already implemented in (1) and (3) to make the diagonal elements or diagonal sub-matrix of $K$ zero.[22] For the 3-channel system,

$$K = \begin{pmatrix} K^{oo} & K^{oc} \\ K^{co} & K^{cc} \end{pmatrix} = \begin{pmatrix} 0 & K_{12} & K_{13} \\ K_{12} & 0 & K_{23} \\ K_{13} & K_{23} & 0 \end{pmatrix} \quad (4)$$

where, o and c label open and closed channels, respectively, In (4), index 1 is for the open channel and 2 and 3 for closed ones in limit interval 2 while indices 1 and 2 are for open channels and index 3 for closed ones in limit interval 3 (see Fig. 1). The same reactance matrix (4) will be used for all limit intervals in order to treat them on the same basis. Otherwise, $K^{oo}$ could have been made to zero matrix in limit interval 3. With (1) and (3), the transition dipole moment can be written in matrix form as;

$$\mathbf{D} = [D^o - D^c(\tan\beta + K^{cc})^{-1}K^{co}]\cos\delta \quad (5)$$

where, $D^c$ denotes $(\Psi^c|T|\Psi_i)$ and $D^o$ is similarly defined. Formulas for the photoionization cross sections can be obtained by substituting (5) with reactance matrices given by (4) into $K|\mathbf{D}|^2$. Although phase renormalization in MQDT was introduced to transparently exhibit resonance structures and was successful for the one-open-one-closed-channel system, it is only the necessary condition not sufficient enough to identify the resonance structures.

For the systems involving 1 open and 2 closed channels, resonance-structures-resolved photoionization cross-sections in the limit interval 2 are obtained by Ueda[18] as follows;

$$\sigma_{II} = KD_1^2\frac{(\varepsilon_3+q_3)^2}{\varepsilon_3^2+1}\frac{(\varepsilon_{2eff}+q_{2eff})^2}{\varepsilon_{2eff}^2+1} \quad (6)$$

(For the resonance-resolvability of the form (6), see Appendix A of Ref. [23].) The sub-index II denotes that it is the cross-section at limit interval 2. The first Beutler-Fano term on the right-hand side of (6) is the autoionization cross-section of the interloper series alone. It serves as an envelope to the second Beutler-Fano term from Rydberg series 2. The line profile index $q_{2eff}$ for the lines of the Rydberg series 2 perturbed by an interloper series 3 is given by[23];

$$q_{2eff} = \frac{q_2\varepsilon_3^2 - (1+q_3k_{23})\varepsilon_3 + k_{23} - q_3 + q_2}{(\varepsilon_3 - k_{23})(\varepsilon_3+q_3)} \quad (7)$$

The reduced energy is defined as $\varepsilon_i = \tan(\beta_i + \pi\mu_i)/K_{1i}^2$ ($i$ = 2, 3) with $\beta_i$ denoting $\pi\nu_i$. $W_{2eff}$ and $\varepsilon_{2eff}$ corresponding to the reduced width $W_2(\equiv K_{12}^2)$ and the reduced energy $\varepsilon_2$ perturbed by an interloper, respectively, are given by:

$$\begin{aligned} W_{2eff} &= W_2\frac{(\varepsilon_3-k_{23})^2}{\varepsilon_3^2+1} \\ \varepsilon_{2eff} &= \frac{W_2}{W_{2eff}}\left[\varepsilon_2 + \frac{\varepsilon_3(1-k_{23}^2)-2k_{23}}{\varepsilon_3^2+1}\right] \end{aligned} \quad (8)$$

where, $k_{23}$ denotes $K_{23}/(K_{12}K_{13})$.

**Cross Section Formulas in Limit Interval 3 in Terms of QDT Parameters in Limit Interval 2.** Now consider cross section formulas in limit interval 3 in terms of QDT parameters in limit interval 2. In limit interval 3, two channels are open and one channel is closed. In this case, it is known that the photoionization cross section can be expressed as,[19]

$$\begin{aligned} \sigma_{III} &= K\left[D_{r1}^2\frac{(\tan(\beta_3+\pi\mu_c)/\xi_r^2+q_r)^2}{1+\tan^2\tilde{\beta}/\xi_r^4} + D_{r2}^2\right] \\ &= K\left[D_{r1}^2\frac{(\varepsilon_r+q_r)^2}{\varepsilon_r^2+1} + D_{r2}^2\right] \end{aligned} \quad (9)$$

where, sub-index III indicates limit interval 3; r in the sub-index will be used to denote the representation in which $\sigma_{III}$ takes the form of (9). This representation will be called r-representation; $D_{r1}$, $D_{r2}$ and $D_{r3}$ are transition dipole moments into channels 1, 2 and 3 in the r-representation; the line profile index $q_r$ denotes $-D_{r3}/(\xi_{r1}D_{r1})$ with the fitting parameter $\xi_r$ related to the reduced spectral width $W_r$ as $W_r = \xi_r^2$ ; the fitting parameter $\mu_c$ denotes the phase shift and is used to define $\varepsilon_r$ as $\tan(\beta_3+\pi\mu_c)/W_r$. In this limit interval, experimental data are routinely fitted to the form (9) and are represented with energy-insensitive QDT parameters $\xi_r$, $I_3$, $\mu_c$ and $D_{ri}$ ($i$ = 1, 2, 3).[24] On the other hand, different QDT parameters $K_{12}$, $K_{13}$ and $K_{23}$, $I_i$, $\mu_i$ ($i$ = 2, 3) and $D_i$ ($i$ = 1, 2, 3) are used to fit the experimental data in limit interval 2.[18,25] (Different fitting procedures to experimental data have also been used. If short-range eigenchannels are available at least approximately, the procedure devised by Lu and Lee provides the powerful systematic approach.[26-28] Molecular systems belong to such a case, but additional steps are needed. The procedure devised by Jungen has been the primarily chosen approach in this case.[29-31]) Obviously, we cannot equate $D_{ri}$ with $D_i$. It is thus desirable to express the QDT parameters in limit interval 3 in terms of the QDT parameters in limit interval 2. Let us tackle this problem by using the theory developed in LK.[19]

Since it is hard to directly obtain the relations between two sets of QDT parameters, LK utilized the intermediate representation, called the tilde representation, which is specified only by two conditions while more conditions are needed to specify the r-representation that yields (9). Two conditions are minimal conditions by which the sum of eigenphases of the physical reactance matrix **K** satisfies the simplest resonance behavior given by;

$$\tan\sum_{j\in \mathrm{P}}\tilde{\delta}_j = -\xi_{\mathrm{r}}^2/\tan\tilde{\beta}_{\mathrm{c}} \tag{10}$$

where, $\tilde{\beta}_{\mathrm{c}}$ denotes the phase shifted $\beta_3(=\pi\nu_3)$ by $\pi\mu_{\mathrm{c}}$, *i.e.*, $\beta_{\mathrm{c}} = \pi(\nu_3+\mu_{\mathrm{c}})$. The parameter with tilde signifies that it is the parameter in the tilde representation. From the general relation $\tan\sum_{j\in \mathrm{P}}(\delta_j-\delta_j^0)[\tan\beta_3-\Re(\kappa^{\mathrm{cc}})] = -\xi^2$ for the sum of eigen-phases, two conditions are obtained as $\sum_{j\in \mathrm{P}}\delta_j^0 = 0$ and $\Re(\kappa^{\mathrm{cc}}) = 0$ where $\delta_j^0$ are the phases of eigenvalues $\tan\delta_j^0$ of $K^{\mathrm{oo}}$ and $\kappa^{\mathrm{cc}}$ is defined by $K^{\mathrm{cc}}-iK^{\mathrm{co}}(1+iK^{\mathrm{oo}})^{-1}K^{\mathrm{oc}}$. The former condition removes phase shifts from background scattering in open channels and the latter one removes the phase shift from background scattering in the closed channel at the intermediate range in which the closed-ness of channels is not determined yet (see Appendix A of Ref. [32] for the latter type of phase shift). The phase shifts due to the avoided cross interaction are removed by considering the sum of phase shifts.[33] This means that $\sum_{j\in \mathrm{P}}\tilde{\delta}_j$ in (10) is equal to the resonance eigenphase $\delta_{\mathrm{r}}$ whereby the reduced resonance energy $\varepsilon_{\mathrm{r}}$ in (9) can be defined by $\varepsilon_{\mathrm{r}} = -\cot\delta_{\mathrm{r}}$. The phase shifts $\mu_\Sigma$ and $\mu_{\mathrm{c}}$ that make two conditions satisfied are given by;

$$\begin{aligned}\tan 2\pi\mu_{\mathrm{c}} &= \frac{2\Re(\kappa^{\mathrm{cc}})}{1-\left|\kappa^{\mathrm{cc}}\right|^2},\\ \tan\pi\mu_\Sigma &= \frac{\mathrm{tr}K^{\mathrm{oo}}+(K^{\mathrm{cc}}\ \mathrm{tr}\ K^{\mathrm{oo}}-\mathrm{tr}\ K^{\mathrm{oc}}\ K^{\mathrm{co}})\tan\pi\mu_{\mathrm{c}}}{1-\left|K^{\mathrm{oo}}\right|+(K^{\mathrm{oo}}-|K|)\tan\pi\mu_{\mathrm{c}}}\end{aligned} \tag{11}$$

where, super-index o denotes channel indices 1 and 2 and c denotes 3 in limit interval 3.

To obtain the remaining QDT parameters $D_{\mathrm{r}i}$ $(i = 1, 2, 3)$ and $\xi_{\mathrm{r}}$, resonance eigenframe should be found. This amounts to finding the particular type of linear combinations of open channels which can interact with the closed channels and the other combinations orthogonal to it which cannot interact with the closed channels, as first pointed out by Fano and Cooper.[34] According to LK, procedures for finding the resonance eigenframe from the tilde representation can be diagrammatically represented as follows[19];

$$\begin{cases}\tilde{K}\\ \Re(\tilde{\kappa}^{\mathrm{cc}})=0\\ \Im(\tilde{\kappa}^{\mathrm{cc}})=-\xi_{\mathrm{r}}^2\\ \mathrm{tr}(\tilde{K}^{\mathrm{oo}})=0\end{cases}\xrightarrow[\text{step 1}]{U^{\mathrm{oo}}=e^{-i\frac{1}{2}\theta_0\sigma_y}}\begin{cases}\overline{\overline{K}}\\ \Re(\overline{\overline{\kappa}}^{\mathrm{cc}})=0\\ \Im(\overline{\overline{\kappa}}^{\mathrm{cc}})=-\xi_{\mathrm{r}}^2\\ \mathrm{tr}(\overline{\overline{K}}^{\mathrm{oo}})=0\end{cases} \tag{12}$$

$$\xrightarrow[\text{step 2}]{\mu^0=\left(\frac{1}{2}\Delta_{12}^0,-\frac{1}{2}\Delta_{12}^0\right)}\begin{cases}\overline{K}\\ \Re(\overline{\kappa}^{\mathrm{cc}})=0\\ \Im(\overline{\kappa}^{\mathrm{cc}})=-\xi_{\mathrm{r}}^2\\ \overline{K}^{\mathrm{oo}}=0\\ \overline{K}^{\mathrm{co}}=(\cos\theta_{\mathrm{r}},\sin\theta_{\mathrm{r}})\end{cases}\xrightarrow[\text{step 3}]{U^{\mathrm{oo}}=e^{-i\frac{1}{2}\theta_{\mathrm{r}}\sigma_y}}\begin{cases}K_{\mathrm{r}}\\ \Re(\kappa_{\mathrm{r}}^{\mathrm{cc}})=0\\ \Im(\kappa_{\mathrm{r}}^{\mathrm{cc}})=-\xi_{\mathrm{r}}^2\\ K_{\mathrm{r}}^{\mathrm{oo}}=0\\ K_{\mathrm{r}}^{\mathrm{co}}=(1,0)\end{cases}$$

where, $\theta_0$ denotes $\tan^{-1}(\tilde{K}_{12}/\tilde{K}_{11})$; $\Delta_{12}^0$ denotes $\tan^{-1}[2\sqrt{\tilde{K}_{11}^2+\tilde{K}_{12}^2}/(1-\tilde{K}_{11}^2-\tilde{K}_{12}^2)]$; $\theta_{\mathrm{r}}$ is given by $\tan^{-1}(2\tilde{K}_{13}\tilde{K}_{23}/(\tilde{K}_{13}-\tilde{K}_{23}))-\theta_0$; $U^{\mathrm{oo}}$ denotes an orthogonal transformation whereby $K^{\mathrm{oo}}$ is transformed to $(U^{\mathrm{oo}})^{\mathrm{T}}K^{\mathrm{oo}}U^{\mathrm{oo}}$, $K^{\mathrm{oc}}$ to $(U^{\mathrm{oo}})^{\mathrm{T}}K^{\mathrm{oc}}$ and $K^{\mathrm{co}}$ to $K^{\mathrm{co}}U^{\mathrm{oo}}$.

The procedure (12) can be visualized by considering a vector space whose constituent vectors are phase shift matrices $\Delta$ defined by $S = \exp(-2i\Delta)$. The vector space formed from the set of matrices or operators is called the Liouville space.[35,36] For the two open-channel-system, phase shift matrices $\Delta$ are 2-by-2 matrices and thus can be spanned by 4 basis vectors 1, $\sigma_x$, $\sigma_y$ and $\sigma_z$ orthogonal to each other in the sense that the trace of their product is zero.[35] But for the visualization of diagram (12), 3-dimensional Liouville space spanned by Pauli matrices $\sigma_i$ $(i = x, y, z)$ is enough since the isotropic part of $\Delta$ is already separated out into (10) thus leaving only the anisotropic part satisfying $\mathrm{tr}(\Delta) = 0$. Let $\Delta$ denote the pure anisotropic phase shift matrix so that $\mathrm{tr}\Delta = 0$. Then it can be written as $\Delta = \sigma\cdot\mathbf{n}$. The vector $\mathbf{n}$ is real since scattering matrix is unitary so that phase shift matrix $\Delta$ is Hermitian. It is called a polarization vector, which plays the role of a quantization axis for the coordinate system, and can thus be used to represent the coordinate system. For the physical scattering matrix, $\mathbf{n}$ is restricted to lying on the xz plane. Let us prove this. A scattering matrix or its phase-shift matrix is symmetric because of the time-reversal symmetry. This means that the anti-symmetric $\sigma_y$ cannot appear in the representation $\sigma\cdot\mathbf{n}$ of $\Delta$. Such a requirement is met only when the y-component of $\mathbf{n}$ is zero, thus $\mathbf{n}$ is restricted to lying on the xz plane. The xz plane in Liouville space can thus be called the physical plane. LK stated that the y component of the quantization axis $\hat{\mathbf{n}}_{\mathrm{r}}$ for the resonance eigenframe is not zero. The $\hat{\mathbf{n}}_{\mathrm{r}}$ is given by $(\sin\theta_{\mathrm{r}}\cos\Delta_{12}^0, -\sin\theta_{\mathrm{r}}\sin\Delta_{12}^0, \cos\theta_{\mathrm{r}})$. This does not contradict the fact that physical $\Delta$ cannot have a y-component since the resonance eigenchannel itself is not directly measured. It is indirectly observed only through $\hat{\mathbf{n}}_{\mathrm{obs}}$ on the physical plane.

Figure 2 shows the process of finding the resonance eigenframe from the reference frame of the tilde representation in the limit interval 3. The tilde representation is represented

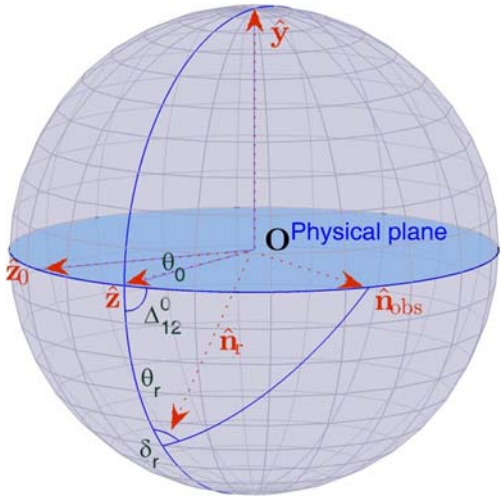


**Figure 2.** Vectors $\hat{\mathbf{z}}_0$, $\hat{\mathbf{z}}$, $\hat{\mathbf{n}}_{\mathrm{r}}$ representing quantization axes of coordinate frames for tilde, double-bar, r-representations in Liouville space. Please refer to the text for the descriptions of parameters.

by $\hat{\mathbf{z}}_0$ in Liouville space.[36] The first step is the orthogonal transformation $\exp(-i\sigma_y\theta_0/2)$ that changes the reference frame to the background eigenframe represented by $\hat{\mathbf{z}}$ by rotation about the y axis by $\theta_0$. The second step is the phase renormalization of regular and irregular base-pair pertaining to channels 1 and 2 by $\Delta_{12}^0/2$ and $-\Delta_{12}^0/2$, respectively. The geometrical transformation corresponding to this step is to remove the background part pertaining to $\Delta_{12}^0$ by rotation of the coordinate system about the z axis by $-\Delta_{12}^0$. The third step is to make this $\hat{\mathbf{n}}_r$ the z axis. The coordinate frame obtained finally is the resonance eigenframe.

The transformation relations between the transition dipole moment elements in the tilde- and r-representations can then be obtained by following the procedures shown diagrammatically in (12):

$$
\begin{aligned}
D_{r1} &= \frac{1}{(1+\tilde{K}_{11}^2+\tilde{K}_{12}^2)^{1/2}}\frac{\tilde{D}_1\tilde{K}_{13}+\tilde{D}_2\tilde{K}_{23}}{(\tilde{K}_{13}^2+\tilde{K}_{23}^2)^{1/2}} \\
D_{r2} &= \frac{1}{(1+\tilde{K}_{11}^2+\tilde{K}_{12}^2)^{1/2}}\frac{-\tilde{D}_1\tilde{K}_{23}+\tilde{D}_2\tilde{K}_{13}}{(\tilde{K}_{13}^2+\tilde{K}_{23}^2)^{1/2}} \\
D_{r3} &= \tilde{D}_3-\frac{\tilde{D}_1(\tilde{K}_{11}\tilde{K}_{13}+\tilde{K}_{12}\tilde{K}_{23})+\tilde{D}_2(\tilde{K}_{12}\tilde{K}_{13}-\tilde{K}_{11}\tilde{K}_{23})}{1+\tilde{K}_{11}^2+\tilde{K}_{12}^2}
\end{aligned}
\tag{13}
$$

Or in terms of the geometrical parameters of Liouville space in Figure 2, they are given by

$$
\begin{aligned}
D_{r1} &= \cos\frac{\Delta_{12}^0}{2}\left(\tilde{D}_1\cos\frac{\theta_r+\theta_0}{2}+\tilde{D}_2\sin\frac{\theta_r+\theta_0}{2}\right) \\
D_{r2} &= \cos\frac{\Delta_{12}^0}{2}\left(-\tilde{D}_1\sin\frac{\theta_r+\theta_0}{2}+\tilde{D}_2\cos\frac{\theta_r+\theta_0}{2}\right) \\
D_{r3} &= \tilde{D}_3-\xi_r\tan\frac{\Delta_{12}^0}{2}(D_{r1}\cos\theta_r-D_{r2}\sin\theta_r)
\end{aligned}
\tag{14}
$$

From (13) or (14), the line profile index $q_r$ defined by $-D_{r3}/(\xi_r D_{r1})$ can be expressed in terms of the transition dipole moment elements in the tilde representation;

$$
q_r=\frac{\tilde{D}_1(\tilde{K}_{11}\tilde{K}_{13}+\tilde{K}_{12}\tilde{K}_{23})+\tilde{D}_2(\tilde{K}_{12}\tilde{K}_{13}+\tilde{K}_{11}\tilde{K}_{23})-\tilde{D}_3(1+\tilde{K}_{11}^2+\tilde{K}_{12}^2)}{\tilde{D}_1\tilde{K}_{13}+\tilde{D}_2\tilde{K}_{23}}
\tag{15}
$$

or

$$
q_r=-\frac{\tilde{D}_3}{\xi_r D_{r1}}+\tan\frac{\Delta_{12}^0}{2}\left(\cos\theta_r-\frac{D_{r2}}{D_{r1}}\sin\theta_r\right)
\tag{16}
$$

Let us finally consider expressing the tilde quantities into the untilde ones. The transformation relations between the transition dipole moment elements in the tilde- and untilde-representations are not uniquely given since the tilde representation is defined with the zero condition of the sum $\pi\Sigma_{j\in P}\mu_j=\Sigma_{j\in P}\delta_j^o$. There are an infinite number of ways of making the sum zero. In the present study, two choices were tried. One choice was to distribute the sum equally to all the components and the other was to make all $\delta_j^0$ but one $\delta_1^0$ zero, *i.e.*, $\pi\mu_j=\delta_\Sigma^0\delta_{j1}$. The latter option was eventually chosen. The relation between the matrix elements of $K$ and $K$ in this choice is obtained as;

$$
\begin{aligned}
\tilde{K}^{oo} &= \frac{-(K_{13}^2\tan\pi\mu_c+\tan\pi\mu_\Sigma)\sigma_z+(K_{12}-K_{13}K_{23}\tan\pi\mu_c)\times\sigma_x/\cos\pi\mu_\Sigma}{1-K_{13}^2\tan\pi\mu_c\tan\pi\mu_\Sigma} \\
\tilde{K}^{co} &= \frac{[K_{13}/\cos\pi\mu_\Sigma\ \ K_{23}-K_{12}K_{13}\tan\pi\mu_\Sigma]}{\cos\pi\mu_c-K_{13}^2\sin\pi\mu_c\tan\pi\mu_\Sigma} \\
\tilde{K}^{cc} &= -\frac{\tan\pi\mu_c+K_{13}^2\tan\pi\mu_\Sigma}{1-K_{13}^2\tan\pi\mu_c\tan\pi\mu_\Sigma}
\end{aligned}
\tag{17}
$$

where, $\sigma_i$ $(i = z, x)$ are Pauli matrices. Similarly, the relation between $\tilde{D}_i$ and $D_j$ is obtained as follows:

$$
\begin{aligned}
\tilde{D}_1 &= D_1(\cos\pi\mu_\Sigma-\sin\pi\mu_\Sigma\tilde{K}_{11})-D_3\sin\pi\mu_c\tilde{K}_{13} \\
\tilde{D}_2 &= D_2-D_1\sin\pi\mu_\Sigma\tilde{K}_{12}-D_3\sin\pi\mu_c\tilde{K}_{23} \\
\tilde{D}_3 &= D_3(\cos\pi\mu_c-\sin\pi\mu_c\tilde{K}_{33})-D_1\sin\pi\mu_\Sigma\tilde{K}_{13}
\end{aligned}
\tag{18}
$$

Eq. (15) with (17) and (18) enables us to calculate $q_r$ in terms of un-tilde QDT parameters and thus our goal is attained.

Interestingly, the reduced width $W_r(=\xi_r^2)$ enjoys a simple relation with the elements of $K$ as follows;

$$
W_r=\frac{W}{1+\tan\pi\mu_c\Re(\kappa^{cc})}
\tag{19}
$$

where, the formula for $\mu_c$ is given in (11) and $W$ is defined by $-\Im(\kappa^{cc})$ and explicitly given by $(K_{13}^2+K_{23}^2)/(1+K_{12}^2)$. The short-range reactance matrix in the final r-representation in (12) is described by $\xi_r$ alone as follows:

$$
K_r=\begin{pmatrix} 0 & 0 & \xi_r \\ 0 & 0 & 0 \\ \xi_r & 0 & 0 \end{pmatrix}
\tag{20}
$$

The form (20) indicates that only $\Psi_{r1}$ between two open channel basis functions $(\Psi_{r1}, \Psi_{r2})$ interacts with the closed channel basis function $\Psi_{r3}$. The channel basis functions $(\Psi_{r1}, \Psi_{r2})$ pertaining to $K_r$ corresponds to 'a' and 'b' states of Fano, or effective continua of Cooke and Cromer.

**Changes in Resonance Eigenframe and Spectral Shape.** Let us consider the continuation problem of the photoionization cross section formulas across the threshold of channel 2 in Figure 1. Recalling that the dynamics in the interloper series is hardly affected by the autoionizing series belonging to lower ionization limit, it might be expected that the interloper spectrum be continued across the threshold and the perturbed autoionizing series now contributes only as a background spectrum insensitive to energy. In order to examine whether this expectation bears out from the quantitative basis, let us consider the simple case of $K_{23} = 0$ in which, $K_{12}$ and $K_{13}$ are the only nonzero elements that can bring about the change in the resonance eigenframe.

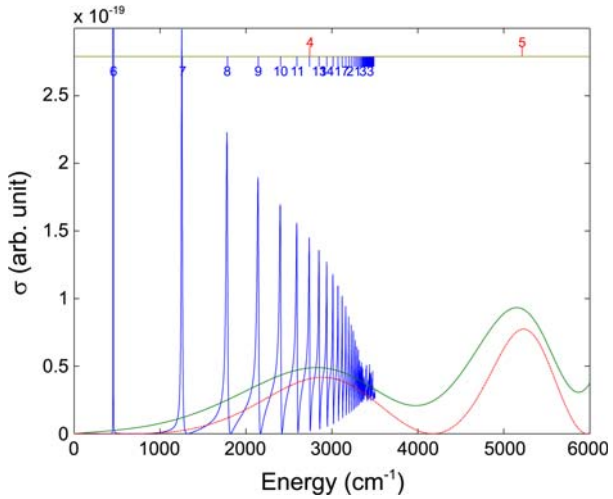


**Figure 3.** The solid smooth curve on the left-hand side of the second threshold is the photoionization cross section averaged over one unit interval of $\nu_2$ and is analytically continued to the cross section above the threshold so that $\langle\sigma_{\rm II}\rangle_{\nu_2} = \sigma_{\rm III}$. The broken curve is the autoionizing spectrum $\sigma_0(\varepsilon_3 + q_3)^2/(\varepsilon_3^2 + 1)$ of interloper series 3 when only the channels 1 and 3 are included. It is usually used as an envelope to the perturbed autoionizing series 2 below the threshold. Nevertheless, it is not continued to the cross section above the threshold. Nonzero parameters used to draw the plot is as follows: $I_2$ = 3500 cm$^{-1}$, $I_3$ = 9600 cm$^{-1}$, $K_{12} = 0.02\pi$, $K_{13} = 0.3\pi$, $K_{23} = 0.1\pi$, $D_1$ = 1 a.u., $D_2$ = 100 a.u., $D_3$ = 150 a.u..

*The case of* $K_{23} = 0$

In this case, there is no need to use the intermediate tilde representation since $\Re(\kappa^{\rm cc}) = 0$ and $\delta_\Sigma^0 = 0$ conditions are already satisfied so that $K$ is equal to $\tilde{K}$ from the outset. In this case, the values $\theta_0$ and $\theta_{\rm r}$ are given by $\pi/2$ and $-\pi/2$, respectively, from their definitions given below (12). The reason why the value of $\theta_0$ is $\pi/2$ comes from the zeros of the diagonal elements of $K^{\rm oo}$ so that the polarization vector for $K^{\rm oo}$ points to x direction since, $K^{\rm oo} = K_{12}\sigma\cdot\hat{\mathbf{x}}$. Subsequently, taking $\theta_0 = \pi/2$ transforms $K_{12}\sigma\cdot\hat{\mathbf{x}}$ to $K_{12}\sigma\cdot\hat{\mathbf{z}}$. Such a simple explanation cannot be given at this moment for the reason why the value of $\theta_{\rm r}$ is $-\pi/2$.

Substituting $\theta_0 + \theta_{\rm r} = 0$ and $\theta_{\rm r} = -\pi/2$ into (14) or $\tilde{K}_{11} = \tilde{K}_{23} = 0$ into (13), $D_{ri} = \cos(\Delta_{12}^0)D_i = D_i/\sqrt{1+K_{12}^2}$ (i = 1, 2) is obtained. It means that the effective continuum wavefunctions $(\Psi_{\rm r1}, \Psi_{\rm r2})$ are proportional to the un-tilde ones as $\Psi_{ri} = \Psi_i \cos(\Delta_{12}^0/2) = \Psi_i/\sqrt{1+W_2}$ ($i$ = 1, 2). Note that $1 + (K^{\rm oo})^2$ is equal to $1 + K_{12}^2$, indicating that the factor $\cos(\Delta_{12}^0/2)$ or $\sqrt{1+K_{12}^2}$ adjusts the change in normalization caused by the newly added open channel 2 so as to make $\Psi_{ri}$ energy-normalized within the subspace composed of open channels. However, this newly added open channel does not affect the orientation of the background eigenframe. The relations between resonance parameters $q_{\rm r}$ and $W_{\rm r}$ in (9) in the limit interval 3 and those in the limit interval 2 are subsequently obtained as;

$$q_{\rm r0} = q_3 + (q_3 - q_2)W_2$$
$$W_{\rm r0} = W_3/(1 + W_2) \quad (\text{when } K_{23} = 0) \tag{21}$$

where, 0 is attached to the sub-indices to stand for $K_{23} = 0$ and the notation $W_2$ is preferred to $K_{12}^2$ if the relevant energy range belongs to limit interval 2. The second equation of (21) tells us that spectral reduced widths are also different by factor of $(1 + W_2)^{-1}$. Since the spectral minimum (maximum) of the Beutler-Fano term takes place at $\varepsilon = -q$ ($1/q$), the spectral minimum of the autoionizing spectrum (9) occurs at $\varepsilon_{\rm r} = -q_{\rm r}$ ($1/q_{\rm r}$) and that of the interloper spectrum $\sigma_0(\varepsilon_3 + q_3)^2/(\varepsilon_3^2 + 1)$ takes place at $\varepsilon_3 = -q_3$ ($1/q_3$). Since $q_{\rm r}$ differs from $q_3$ by $(q_3 - q_2)W_2$ according to the first equation of (21), the minima (maxima) of both spectra do not coincide in general.

Let us consider the effect of change in resonance frames on the optimum values of cross sections. The minimum of cross sections is zero in limit interval 2. Cross sections are not zero at the minimum in limit interval 3, however, because of the contribution from the background scattering. From (9), the background term given by $KD_{\rm r2}^2$ or $KD_2^2/(1+K_{12}^2)$ is contributed from the newly added open channel with the correction factor $1+K_{12}^2$ for the change in normalization due to the newly added open channel. Let us consider the maximum value. Using the fact that the maximum value of Beutler-Fano term $(\varepsilon+q)^2/(\varepsilon^2+1)$ is given by $q^2+1$ at $\varepsilon = 1/q$, the maximum value of the interloper spectrum $KD_1^2(\varepsilon_3+q_3)^2/(\varepsilon_3^2+1)$ is obtained as $KD_1^2(q_3^2+1) = {\rm K}(D_3^2/W_3 + D_1^2)$. For the autoionizing spectrum (9), the maximum is given by $\sigma_{\rm III,max} = K[D_{\rm r1}^2(q_{\rm r0}^2+1) + D_{\rm r2}^2]$. Substituting $D_{ri} = D_i\cos(\Delta_{12}^0/2)$ ($i$ = 1, 2) and $q_{\rm r0} = -D_3/(\xi_{\rm r}D_{\rm r1}) + \tan(\Delta_{12}^0/2)(D_2/D_1)$ into $\sigma_{\rm III,max}$, we obtain;

$$\sigma_{\rm III,max} = K\left[\frac{D_3^2}{W_{\rm r}} + D_2^2 + D_1^2\cos^2\left(\frac{\Delta_{12}^0}{2}\right) - 2\frac{D_2D_3}{\xi_{\rm r}}\sin\left(\frac{\Delta_{12}^0}{2}\right)\right] \tag{22}$$

Note that $\sin\Delta_{12}^0$ is given by $2K_{12}/(1+K_{12}^2)$. If there is no channel coupling between the existing open channel and the newly added open channel so that $K_{12} = 0$, then the interference term between channels 2 and 3 becomes zero and $\sigma_{\rm III,max}$ becomes $K[D_3^2(1+K_{12}^2)/W_3 + D_2^2 + D_1^2]$, which is equal to the sum of the maximum of interloper spectrum and the background one contributed from the newly added open channel 2 except for the normalization-adjusting factor $1+K_{12}^2$ multiplying $D_3^2$ term.

*The case of* $K_{23} \neq 0$

Let us now lift the restriction so that $K_{23}$ is not zero in general. Since channel coupling between channels 2 and 3 is no longer zero, conversion of channel 2 from closed to open channel when the threshold is crossed now reduces the dimension of the space consisting of closed channels. This change raises a new problem of positioning of the resonance to the origin of the eigenframe. The phase shifts given in (11) reposition the resonance to the origin of the eigenframe so that the simplest resonance relation (10) holds again. Then the effect of newly added open channel on the existing open channel can be dealt with in this resonance centered tilde representation. In this case, the picture obtained in the case of $K_{23} = 0$ may be applied with only minor modifications. Corresponding formula for (22) is obtained as follows;

$$\sigma_{\mathrm{III,max}} = K\begin{bmatrix} \frac{\tilde{D}_3^2}{W_r}+\tilde{D}_1^2+\tilde{D}_2^2-\tan^2\left(\frac{\Delta_{12}^0}{2}\right)(D_{r1}\sin\theta_r+D_{r2}\cos\theta_r)^2 \\ -2\frac{\tilde{D}_3}{\xi_r}\tan\left(\frac{\Delta_{12}^0}{2}\right)(D_{r1}\cos\theta_r-D_{r2}\sin\theta_r) \end{bmatrix} \quad (23)$$

The difference between (23) and (22) arises because the value of $\theta_r$ is no more given as a right angle so that, instead of a single term of $D_{ri}$, their combinations appear. In addition, a modification to the normalization factor is needed for the case of $K_{23}\neq 0$ coming from additional coupling term between the newly added open channel and the existing one. That is the product between two diagonal elements of $\tilde{K}^{oo}$ given by $\tilde{K}_{11}\tilde{K}_{22} = -\tilde{K}_{11}^2$. Because of this factor, $\sin\Delta_{12}^0$ is modified to $2\sqrt{\tilde{K}_{11}^2+\tilde{K}_{12}^2}/(1+\tilde{K}_{11}^2+\tilde{K}_{12}^2)$.

**Analytical Continuation of Photoionization Cross Section at Thresholds.** In the previous section, we examined the continuation of an interloper spectrum as the threshold is crossed. Actually, similar kind of problem of analytical continuation was treated by Fonda and Newton[37] and Gailitis.[15] They showed that the average values of the total scattering cross sections below threshold are analytically continued to the values above threshold in the Coulomb field. Such a continuity is known as Gailitis theorem and was proven to hold for the reactions X (a, $b_f$) $Y_f$ (f=1,…,d) near the threshold of a new reaction X (a, $b_t$) $Y_t$. The theorem is expected to hold for the photoionization cross section since photoionization can be viewed as belonging to such a type of reaction if light is treated as a collection of photon. Nevertheless, direct confirmation of Gailitis theorem in the context of photoionization was repeated in the past[10,13] since it can be done directly with simple mathematics while the derivation in Gailitis's work[15] relies on the results obtained from a large number of preceding papers. But the direct confirmation has been restricted to the system in which all the channels are open above the threshold except for the one by Dubau and Seaton.[14,38] They proposed to use a contracted scattering matrix to treat the effects due to higher thresholds. Here, we will consider averaging the photoionization cross section of autoionizing Rydberg series in the presence of an interloper series, for which no papers doing direct integration has been found yet. For the calculation of the average of the cross section (6) by direct integration, it may be more convenient to express (6) into the form that Wintgen and Friedlich have obtained,[39]

$$\sigma_{\mathrm{II}} = \sigma_0\frac{\varepsilon_2\varepsilon_3+(\varepsilon_2-k_{23})q_3+(\varepsilon_3-k_{23})q_2-k_{23}^2}{(\varepsilon_2\varepsilon_3-k_{23}^2)+(\varepsilon_2+\varepsilon_3-2k_{23})^2} \quad (24)$$

Let us change the integral variable from $\nu_2'(=\nu_2+\mu_2)$ to $x=\tan\pi\nu_2'$ so that $\int_0^1 d\nu_2' = \int_{-\infty}^{\infty} dx/(1+x^2)$. Then taking the upper half complex plane as a contour and then applying the residue theorem to the simple poles at

$$\frac{[2k_{23}+\varepsilon_3k_{23}^2-\varepsilon_3+\mathrm{i}(\varepsilon_3-k_{23})^2]W_2}{1+\varepsilon_3^2},\ +\mathrm{i} \quad (25)$$

we obtain;

$$\frac{\langle\sigma_{\mathrm{II}}\rangle_{\nu_2}}{\sigma_0} = \frac{\begin{matrix}(1+W_2)(1+W_2q_2^2)\varepsilon_3^2+2q_{r0}\varepsilon_3+q_3^2 \\ +W_2(q_3-q_2)^2-2W_2k_{23}\varepsilon_3 f+W_2k_{23}g\end{matrix}}{[(1+W_2)\varepsilon_3-2W_2k_{23}]^2+(1+W_2k_{23}^2)^2} \quad (26)$$

where, $q_{r0}$ is defined in (21) and

$$\begin{aligned} f &= (1+W_2)q_2q_3+1+W_2q_2^2+k_{23}W_2q_2 \\ g &= 2(q_2-q_3)+k_{23}[1+q_3^2+W_2(q_2+q_3)^2] \\ &\quad +2k_{23}^2W_2(q_2+q_3)+W_2k_{23}^3 \end{aligned} \quad (27)$$

Eq. (26) is numerically shown to be identical with (9), *i.e.*, $\langle\sigma_{\mathrm{II}}\rangle_{\nu_2} = \sigma_{\mathrm{III}}$. Note that because of the averaging process, the formula (26) does not go to zero once in every unit interval of $\nu_2$. If only one open channel is involved, cross section should be zero at least once in every unit interval. Since $\langle\sigma_{\mathrm{II}}\rangle_{\nu_2}$ does not go to zero, it can be compatible with $\langle\sigma_{\mathrm{II}}\rangle_{\nu_2} = \sigma_{\mathrm{III}}$ since $\sigma_{\mathrm{III}}$ does not go to zero because there are two open channels in the limit interval 3. In contrast to the simple form of $\sigma_{\mathrm{III}}$, the form of $\langle\sigma_{\mathrm{II}}\rangle_{\nu_2}$ is complicated. From this, it can be argued that cross section formulas take the simpler form when they are expressed in terms of the resonance parameters. The simplicity may be derived from that the resonance and background scatterings are fundamental processes having the simplest behaviors because of their pure nature. Resonance parameters are likely the parameters obtained from experimental data fitting.

Let us consider the next analytical continuation for the third threshold for the completeness. For the integration of $\sigma_{\mathrm{III}}$ of (9) over the unit interval of $\nu_3$, let us denote $\tan\pi(\nu_3+\mu_3+\mu_e)$ as $x$. Then, $\varepsilon_r = W_r x$ and $\pi d\nu_3 = dx/(1+x^2)$. $\langle\sigma_{\mathrm{III}}\rangle_{\nu_3}$ is obtained as follows:

$$\begin{aligned} \langle\sigma_{\mathrm{III}}\rangle_{\nu_3} &= K\left[\frac{W_r}{\pi}\int_{-\infty}^{\infty}\frac{(\varepsilon_r+q_r)^2}{(\varepsilon_r^2+1)(1+W_r^2\varepsilon_r^2)}d\varepsilon_r + D_{r2}^2\right] \\ &= K\left(\frac{D_{r1}^2+D_{r3}^2}{1+W_r}+D_{r2}^2\right) \end{aligned} \quad (28)$$

This should be equal to $\sigma = D(1+K^2)^{-1}D^{\mathrm{T}}$ obtained directly for the system with all the 3 channels open where $D$ denotes ($D_1$ $D_2$ $D_3$) and $K$ denotes (4). The equality is difficult to show because of the complexity of the involved formulas and only confirmed numerically. The formula $\sigma = D(1+K^2)^{-1}D^{\mathrm{T}}$ becomes very complicated when it is expanded in terms of MQDT parameters obtained by data fitting in limit interval 2. In this limit interval, the formula (28) is the simplest one if the QDT parameters obtained by data fitting in the limit interval 3 are used. Once again, we see that the representations suitable for one limit interval may not be suitable in other limit intervals.

**Contracted Basis Sets for the Proof of Analytical Continuity of a Cross Section.** We have seen that it is very difficult to prove directly $\langle\sigma_{\mathrm{II}}\rangle_{\nu_2} = \sigma_{\mathrm{III}}$ without the help from machine. Dubau and Seaton proposed to use a contracted

base set to prove such an equality by eliminating the effects of higher thresholds. With this contracted set, 3-channel systems can be contracted into the 2-channel systems for which the proof of the equality may be easily done. Let us explore this possibility.

In Seaton's contracted matrix method, effects of higher thresholds are eliminated using a contracted matrix. All the structures observed in a restricted range of lower energies may then be accounted for using a small contracted matrix. In the contracted matrix method, the boundary condition that the coefficients of the exponentially rising terms in basis functions for closed channels be zero is applied in two steps. At first, it is applied to eliminate the channels of higher thresholds. Let the set of channels of higher thresholds be labeled as 'b' and the set of other channels be labeled as 'a'. Channels belonging to b are then eliminated in the channel basis functions and reactance matrices using the same method as used in eliminating closed channels:

$$\Psi_a^{(c)} = \Psi_a - \Psi_b(\tan\beta^b + K^{bb})^{-1}K^{ba}$$
$$K^{(c)} = K^{aa} - K^{ab}(\tan\beta^b + K^{bb})^{-1}K^{ba} \quad (29)$$

For the present 2-closed-1-open-channel system, the standing wavefunction $\Psi_3$ pertaining to the higher threshold corresponds to$\Psi_b$ and is contracted into the channel wave functions $\Psi_i$ ($i$ = 1, 2) belonging to $\Psi_a$. From (4), we obtain;

$$\Psi_i^{(c)} = \Psi_i - \frac{\Psi_3}{\tan\beta_3}K_{3i} \quad (i = 1, 2) \quad (30)$$

where, the super-index (c) stands for the contraction. The same notational convention will be kept below for other quantities. In limit interval 2, channel 2 is closed. By making zero of the coefficient of the exponentially rising term, the physical wavefunction is obtained as;

$$\mathbf{\Psi}^{(c)} = \left(\Psi_1^{(c)} - \frac{\Psi_2^{(c)}}{\tan\beta_2 + K_{22}^{(c)}}K_{12}^{(c)}\right)\cos\delta^{(c)} \quad (31)$$

where, the short-range contracted reactance matrix $K^{(c)}$ is defined in (29) and the cosine term is obtained from the physical reactance matrix $\mathbf{K}^{(c)}(=\tan\delta^{(c)})$ as;

$$\cos^2\delta^{(c)} = \frac{1}{1+\mathbf{K}^{(c)2}} = \frac{(\tan\beta_2 + K_{22}^{(c)})^2}{(\tan\beta_2 + K_{22}^{(c)})^2 + (K_{11}^{(c)}\tan\beta_2 + |K^{(c)}|)^2} \quad (32)$$

The square of the modulus of $\mathbf{D}^{(c)}[=(\mathbf{\Psi}^{(c)}|T|i)]$ is then obtained as;

$$|\mathbf{D}^{(c)}|^2 = |D_1^{(c)}|^2 \frac{\left|\frac{\tan\beta_2 + K_{22}^{(c)}}{K_{12}^{(c)2}} - \frac{D_2^{(c)}}{K_{12}^{(c)}D_1^{(c)}}\right|^2}{\left(\frac{\tan\beta_2 + K_{22}^{(c)}}{K_{12}^{(c)2}}\right)^2 + \left(K_{11}^{(c)}\frac{\tan\beta_2 + K_{22}^{(c)}}{K_{12}^{(c)2}} - 1\right)^2} \quad (33)$$

The average of $|\mathbf{D}^{(c)}|^2$ over the unit interval of $\nu_2$ can be easily obtained as;

$$\langle\sigma_{II}^{(c)}\rangle_{\nu_2} = \langle|\mathbf{D}^{(c)}|^2\rangle_{\nu_2} = \int_0^1 |\mathbf{D}^{(c)}|^2 d\nu_2$$
$$= \frac{(1+(K^{(c)2})_{22})D_1^{(c)2} + (1+(K^{(c)2})_{11})D_2^{(c)2} - 2(K^{(c)2})_{12}D_1^{(c)}D_2^{(c)}}{|K^{(c)}|^2 + 1 + K_{11}^{(c)2} + K_{12}^{(c)2} + K_{22}^{(c)2}} \quad (34)$$

Similarly, $\sigma_{III}^{(c)}$ can be obtained from $D^{(c)}(1+K^{(c)2})^{-1}D^{(c)T}$ with $D^{(c)} = (D_1^{(c)}\ D_2^{(c)})$, which yields the same formula as (34), thus proving the relation $\langle\sigma_{II}\rangle_{\nu_2} = \sigma_{III}$. (Note that $\sigma_{II}^{(c)} = \sigma_{II}$ and $\sigma_{III}^{(c)} = \sigma_{III}$) Although the contracted base set is convenient to prove the analytical continuation, the form of the cross section derived from it is not the form used to fit the experimental data.

## Results and Discussion

The MQDT is a powerful theory that describes the complex spectra including energy regions both below and above the threshold with a small number of parameters. Usually the energy dependence of such parameters can be ignored and excellent reproduction of the observed spectra is obtained. If the energy dependence cannot be ignored, only minor modifications of the parameters are enough to obtain the excellent fit to the experimental data. Such an excellent fit to spectra at both sides of a threshold is possible with a single set of QDT parameters since QDT parameters represent the dynamics taking place at short-ranges, where potential is so strong that minor energy variation can be ignored and thus can be used at both sides. Thus, QDT parameters obtained in one limit interval can simultaneously be used to simulate the photoionization spectra in other limit interval. Practically, however, if the spectra can be fitted by Beutler-Fano function, that function is used to fit the spectra instead of using MQDT. This situation takes place since it is better to describe the spectra using the formulas expressed in terms of resonance structures instead of raw MQDT parameters if the resonance structure of the system is known. Superiority of using resonance parameters lies in that resonance and background scatterings are fundamental processes having the simplest behaviors because of their pure nature. In contrast to the raw short-range QDT parameters, resonance parameters are different for different limit intervals because of the different resonance eigenframes for different limit intervals. This raises the problem of finding the relations between different resonance eigenframes for different limit intervals. In the present study, 3-channel systems are chosen to study this problem. In this case, only two limit intervals 2 and 3 in table 1 have resonance eigenframes and need to be considered.

Conversion of channel 2 from closed to open channel, when the second threshold is crossed now reduces the dimension of the space consisting of closed channels. Because of this change, we have new problem of relocating the resonance position to the origin of the eigenframe by shifting the phase shifts by $\pi\mu$ so that the simplest resonance relation $\delta_r = -\xi_r^2/\tan\pi(\nu+\mu)$ holds again. Then the channel coupling effect of newly added open channel on the existing

open channel can be described in this resonance centered representation. If there is no channel coupling between the existing open channel and the newly added open channel, the spectrum is equal to the sum of the interloper spectrum and the background one due to the newly added open channel 2 except for the normalization factor that enters due to the newly added open channel. The newly added open channel also cause change in the orientation of the resonance eigenframe. Putting these effects into consideration, the relations between different resonance eigenframes are obtained.

The formula for the average $\langle \sigma_{II} \rangle_{\nu_2}$ of autoionization cross-section is also obtained in terms of the QDT parameters in the limit interval 2 by integrating directly over the resonance structures in the presence of an interloper series that converge to the second ionization threshold. We confirm that the formula satisfies Gailitis' theorem $\langle \sigma_{II} \rangle_{\nu_2} = \sigma_{III}$. We hope this formula provides experimentalists an additional tool to analyze the autoionization spectra besides Ueda's one, in particular. The complexity of the formula of $\langle \sigma_{II} \rangle_{\nu_2}$ when expressed in terms of QDT parameters in limit interval 2 also makes it clearer that cross section formulas take the simplest form when they are expressed in the resonance eigenframes so that resonance structures are clearly revealed.

We also employed Dubau and Seaton's contracted matrix method to analytically prove $\langle \sigma_{II} \rangle_{\nu_2} = \sigma_{III}$. Although the contracted matrix method is convenient to prove the analytical continuation, the form of the cross section derived from it is found not to be suitable to fit the experimental data. However, the method has many advantages and interesting aspects. We expect it to play a crucial role for further development of MQDT in the near future.

Using the theory developed in this study, it may be worth while to analyze the patterns of changes in resonance eigenframes in real systems. Unfortunately, there seems to be no study of the relations between resonance dynamics above and below thresholds in photoionization of the real systems except for the analytical continuation of cross sections. We hope the present study spurs research in this direction.

Final comment is that since energy range including several thresholds is considered in the present study, the energy dependence of QDT parameters may not be ignored. Thus, caution is needed when applying the formulas obtained in the present study. In the neighborhood of thresholds, analytically continued formulas will have no problem but far from the thresholds, $\langle \sigma_{\text{below}} \rangle_{\nu_{\text{bdlow}}} = \sigma_{\text{above}}$ may not be used without including the energy dependence of QDT parameters. How far from the threshold the analytically continued formulas can be applied and how the formulas are modified when the energy dependence of QDT parameters are included are left as a future research topic.

**Acknowledgments.** This study was supported by the Basic Science Research Program through the National Research Foundation of Korea (NRF) funded by the Ministry of Education, Science and Technology (2011-0024808). This study was also supported by an Ajou University Research Fellowship of 2011.

## References

1. Sadeghpour, H. R.; Bohn, J. L.; Cavagnero, M. J.; Esry, B. D.; Fabrikant, I. I.; Macek, J. H.; Rau, A. R. P. *J. Phys. B* **2000**, *33*, R93.
2. Barrachina, R. O. *Nucl. Instrum. Methods Phys. Res., Sect. B* **2005**, *233*, 19.
3. Lindahl, A. O.; Hultgrena, H.; Kiyan, I. Y.; Pegg, D. J.; Rohlen, J.; Walterd, C. W.; Hanstorp, D. *J. Phys. C. Conference Series* **2011**.
4. Wigner, E. P. *Phys. Rev.* **1948**, *73*, 1002.
5. James, S. *et al. Journal of Physics: Conference Series* **2011**, *262*, 012056.
6. Gallup, G. A.; Fabrikant, I. I. *Phys. Rev. A* **2007**, *75*, 032719.
7. Smith, J. R.; Kim, J. B.; Lineberger, W. C. *Phys. Rev. A* **1997**, *55*, 2036.
8. Lineberger, W. C.; Woodward, B. W. *Phys. Rev. Lett.* **1970**, *25*, 424.
9. Fano, U.; Cooper, J. W. *Rev. Mod. Phys.* **1968**, *40*, 441.
10. Seaton, M. J. *Rep. Prog. Phys.* **1983**, *46*, 167.
11. Fano, U.; Rau, A. R. P. *Atomic Collisions and Spectra*; Academic: Orlando, U.S.A., 1986.
12. Landau, L. D.; Lifshits, E. M. *Quantum Mechanics: Non-relativistic Theory*, 3d ed.; Pergamon Press: Oxford; New York, 1977.
13. Fano, U. *Phys. Rev. A* **1970**, *2*, 353.
14. Dubau, J.; Seaton, M. J. *J. Phys. B* **1984**, *17*, 381.
15. Gailitis, M. *Soviet Physics-JETP* **1963**, *17*, 1328.
16. Connerade, J. P. *Proc. R. Soc. London, Ser. A* **1978**, *362*, 361.
17. Cooke, W. E.; Cromer, C. L. *Phys. Rev. A* **1985**, *32*, 2725.
18. Ueda, K. *Phys. Rev. A* **1987**, *35*, 2484.
19. Lee, C.-W.; Kim, J.-H. *Bull. Korean Chem. Soc.* **2002**, *23*, 1560.
20. Lee, C.-W. *J. Phys. B* **2011**, *44*, 195005.
21. Lee, C. W. *Phys. Rev. A* **2002**, *66*, 052704/1.
22. Giusti-Suzor, A.; Fano, U. *J. Phys. B* **1984**, *17*, 215.
23. Lee, C.-W. *Bull. Korean Chem. Soc.* **2010**, *31*, 3201.
24. Maeda, K.; Ueda, K.; Aymar, M.; Matsui, T.; Chiba, H.; Ito, K. *J. Phys. B* **2000**, *33*, 1943.
25. Hieronymus, H.; Neukammer, J.; Rinneberg, H. *J. Phys. B* **1992**, *25*, 3463.
26. Lu, K. T. *Phys. Rev. A* **1971**, *4*, 579.
27. Lee, C. M.; Lu, K. T. *Phys. Rev. A* **1973**, *8*, 1241.
28. Weber, J. M.; Ueda, K.; Klar, D.; Kreil, J.; Ruf, M. W.; Hotop, H. *J. Phys. B* **1999**, *32*, 2381.
29. Jungen, C.; Atabek, O. *J. Chem. Phys.* **1977**, *66*, 5584.
30. Du, N. Y.; Greene, C. H. *J. Chem. Phys.* **1986**, *85*, 5430.
31. Xu, E. Y.; Helm, H.; Kachru, R. *Phys. Rev. A* **1989**, *39*, 3979.
32. Lee, C.-W. *Bull. Korean Chem. Soc.* **2009**, *30*, 891.
33. Lee, C. W. *Phys. Rev. A* **1998**, *58*, 4581.
34. Fano, U.; Cooper, J. W. *Phys. Rev.* **1965**, *137*, A1364.
35. Fano, U. *Rev. Mod. Phys.* **1957**, *29*, 74.
36. Lee, C. W. *Physics Essays* **2000**, *13*, 206.
37. Fonda, L.; Newton, R. G. *Annals of Physics* **1959**, *7*, 133.
38. Yan, Y.; Seaton, M. J. *J. Phys. B* **1987**, *20*, 6409.
39. Wintgen, D.; Friedrich, H. *Phys. Rev. A* **1987**, *35*, 1628.